PNAS RESEARCH ARTICLE | IMMUNOLOGY AND INFLAMMATION

Early age–related atrophy of cutaneous lymph nodes precipitates an early functional decline in skin immunity in mice with aging

Sandip Ashok Sonar[a,b], Jennifer L. Uhrlaub[a,b], Christopher P. Coplen[a,b], Gregory D. Sempowski[c], Jarrod A. Dudakov[d], Marcel R. M. van den Brink[e], Bonnie J. LaFleur[f], Mladen Jergović[a,b], and Janko Nikolich-Žugich[a,b,f,1]

Edited by Marc Jenkins, University of Minnesota Medical School, Minneapolis, MN; received November 23, 2021; accepted March 9, 2022

Secondary lymphoid organs (SLOs) (including the spleen and lymph nodes [LNs]) are critical both for the maintenance of naive T (T_N) lymphocytes and for the initiation and coordination of immune responses. How they age, including the exact timing, extent, physiological relevance, and the nature of age-related changes, remains incompletely understood. We used "time stamping" to indelibly mark newly generated naive T cells (also known as recent thymic emigrants) (RTEs) in mice, and followed their presence, phenotype, and retention in SLOs. We found that SLOs involute asynchronously. Skin-draining LNs atrophied by 6 to 9 mo in life, whereas deeper tissue-draining LNs atrophied by 18 to 20 mo, as measured by the loss of both T_N numbers and the fibroblastic reticular cell (FRC) network. Time-stamped RTEs at all ages entered SLOs and successfully completed postthymic differentiation, but the capacity of older SLOs to maintain T_N numbers was reduced with aging, and that trait did not depend on the age of T_Ns. However, in SLOs of older mice, these cells exhibited an emigration phenotype ($CCR7^{lo}S1P1^{hi}$), which correlated with an increase of the cells of the same phenotype in the blood. Finally, upon intradermal immunization, RTEs generated in mice barely participated in de novo immune responses and failed to produce well-armed effector cells detectable in blood as early as by 7 to 8 mo of age. These results highlight changes in structure and function of superficial secondary lymphoid organs in laboratory mice that are earlier than expected and are consistent with the long-appreciated reduction of cutaneous immunity with aging.

T cells | homeostasis | aging | secondary lymphoid organs

Significance

Older adults are more vulnerable to infection and less capable of vigorously responding to vaccination. The contribution of peripheral T cell maintenance defects to these processes is incompletely understood. Here, we provide evidence that lymph nodes (LNs), which are critical for naive T (T_N) cell maintenance and initiation of new immune responses, age asynchronously. Skin-draining LNs undergo early (6 to 9 mo) and deeper LN and spleen late-life (18 mo) atrophy, characterized by reduced ability to maintain T_N cells, structural and numerical loss of LN stromal cell microenvironments, and reduced immunity to cutaneous vaccination. These results highlight the critical role of age-related LN atrophy in functional immunity and immune homeostasis.

Naive T (T_N) cells are critically important for mounting de novo immune responses against emerging and reemerging pathogens, due to their broad TCR repertoire diversity and consequent specificity for a wide array of antigens. Ontogenically, T_N cells are produced and released by the thymus and then transported by blood and lymph to seed secondary lymphoid organs (SLOs) (in this manuscript, spleen and lymph nodes [LNs]). Such cells are called recent thymic emigrants (RTEs) (1), a definition usually applied to the cells in the first 7 to 14 d following thymic egress. RTEs have characteristic phenotypic and functional features that make them distinct from T_N cells, including high threshold for T cell receptor (TCR) activation, high expression of anergy-related genes, and lower cytokine production capability upon stimulation as compared to mature T_N cells (2). However, RTEs are known to produce a comparable effector response to fully mature T_N cells under inflammatory conditions and upon infectious challenge in mice (3). A series of seminal studies led to a model whereupon successful exit from the thymus, RTEs migrate to the SLO and interact with both stromal and migrating myeloid cells (e.g., dendritic cells [DCs]) that provide further signals leading to their final maturation into T_N cells (2, 4). It simultaneously became clear that SLOs are the key sites that maintain the T_N cell pool under homeostatic and other conditions, including inflammation, infection, and lymphodepletion (5–8). Therefore, homeostatic maintenance of the T_N cell pool largely depends on the balance between seeding and retention of RTEs, long-term maintenance of the new and existing T_N cells in the SLOs, and their loss due to phenotypic transition into other subsets as a consequence of antigenic stimulation, altered maintenance, or death. This ensures that T_N cell numbers, diversity, and function are maintained for long time periods in the SLOs, especially after thymic involution (9, 10). However, homeostatic maintenance of T_N cells deteriorates with advanced age, pronouncing the impairment of protective immunity in older adults (11, 12).

Stromal cells of the SLOs consist of many different cell types of nonhematopoietic origin, which not only provide the overall structural scaffolding of the SLOs, but more

Author contributions: S.A.S., J.L.U., G.D.S., J.A.D., M.R.M.v.d.B., and J.N.-Ž. designed research; S.A.S., J.L.U., C.P.C., and M.J. performed research; S.A.S., C.P.C., B.J.L., and J.N.-Ž. analyzed data; S.A.S. and J.N.-Ž. wrote the paper; and J.N.-Ž. conceived the project and supervised the study.

Competing interest statement: J.N.-Ž. is co-chair of the scientific advisory board of and receives research funding from Young Blood Institute (YBI), Inc. YBI, Inc. had no influence on any aspect of this work or the present manuscript.

This article is a PNAS Direct Submission.

[1]To whom correspondence may be addressed. Email: nikolich@arizona.edu.

This article contains supporting information online at http://www.pnas.org/lookup/suppl/doi:10.1073/pnas.2121028119/-/DCSupplemental.

Published April 19, 2022.

importantly organize themselves into a number of specialized microenvironments (or niches) that play critical roles in lymphocyte maintenance and function (13). For example, fibroblastic reticular cells (FRCs) form a network of reticular conduits coated by extracellular matrix (ECM) that provide homeostatic signals to T_N cells in the form of IL-7 deposited on the ECM and serve as "superhighways" to direct incoming DCs and T_N cells to one another during the initiation of an immune response. Recent studies from some (5, 14–16) but not other (17) groups have suggested that age-related structural deterioration in SLOs might hamper the maintenance and function of T_N cells in old mice. Specifically, Becklund et al. (5) showed that in the steady, homeostatic state, the superficial LNs of the old recipient mice exhibited a defect in the maintenance of young donor $CD4^+$ and $CD8^+$ T cells upon adoptive transfers. This correlated to a numerical reduction in FRCs and reduced connectivity of the FRC network in the T cell zone, which could potentially reduce the bioavailability/access to survival signals, such as IL-7, as well as to a loss in demarcation between T and B cell zones in the LNs (5). These results were corroborated and extended by our group to describe an even more pronounced age-related numerical reduction in lymphatic endothelial cells (LECs) (14). A similar deterioration in T and B cell zone organization and altered T/B interactions have also been reported in human lymph nodes (18). With regard to initiation of new immune responses, old superficial LNs fail to expand in response to West Nile virus (WNV) (16) and chikungunya virus (CHIKV) (19) infections, resulting in reduced T and B cell accumulation, fewer germinal centers, and reduced levels of neutralizing antibodies (16, 19). In the case of WNV, Richner et al. showed that immigrant T and B cells exhibit an age-related delay in entry as well as slow and apparently disorganized migration within the LNs (16), consistent with the disorganization of the FRC network architecture. On the other hand, Masters et al. (17) reported data that confirmed some, but not all, of these results. Specifically, they found age-related changes that affected the architecture and organization of the LNs, erosion of the splenic gp38/podoplanin$^+$ (a FRC marker) area, reduction in T cell zone FRC (also called T cell zone reticular cells [TRCs]) numbers, as well as reduced levels of CCL19 and CCL21 per milligram of total protein (17, 20). However, they also reported that at a steady state, popliteal LNs (superficial) and lung-draining (deep) mediastinal LNs of young and old mice had similar numbers of stromal cells, but that upon influenza infection the proliferation and expansion of the major stromal cell subsets (FRCs [$CD45^-gp38^+CD31^-$], LECs [$CD45^-gp38^+CD31^+$], and blood endothelial cells [BECs] [$CD45^-gp38^-CD31^+$]) of the old mediastinal LNs appeared delayed compared to young counterparts (17). While these results collectively indicate some level of SLO dysfunction with aging, whether and to what extent these age-related LN structural and stromal changes contribute to defects in the maintenance and function of T_N cells remain incompletely understood.

The pool of T_N cells is continuously maintained by a balancing influx of newly generated RTEs and the homeostatic regulation of the mature T_N compartment in SLOs. A cross-sectional analysis of RTEs using Rag-2-pGFP mice revealed that GFP^+ RTEs in the spleen started declining around 24 to 25 wk of age and remained stable thereafter (21). However, in that model, thymocytes were labeled by GFP expressed off the episomal circles generated during V(D)J recombination, and the label is relatively rapidly lost following exit from the thymus (typically within a week of egress). This disallows studies of cohorts of T cells born at different ages or their prolonged followup in the postthymic period in SLOs. Because residual thymic output remains even at older ages, it is important to understand the biology of the RTEs generated de novo in old age and to compare them to those generated earlier in life. For these reasons, the ability of newly generated RTEs to seed, survive, and be maintained in the peripheral LNs (pLNs) at different ages has not been systematically investigated. Zhang et al. elegantly solved the technical limitations of this problem, by stably marking distinct waves of T cells using the tamoxifen-driven TCRδCre.ER-ZsGreen–inducible labeling (22). They followed T cells generated at early (1 mo) and late (16 mo) life and found that labeled T cells in SLOs were mainly of naive and memory phenotype, at 3 and 18 mo of age, respectively (22), consistent with other work in the field (reviewed in ref. 11).

To further address the timing, the extent, and physiological importance of age-related SLO defects, including disturbances in SLO stromata, we deployed the above TCRdCre.ER mouse model (22) (generously provided by Y. Zhuang, Duke University, Durham, NC), which allowed us to "time stamp" label distinct waves of newly generated RTEs at different chronological ages. We report a surprisingly early decline (6 to 9 mo) of RTEs in the skin-draining (axillary and inguinal) LNs, whereas the deeper SLOs (e.g., brachial LNs and spleen) exhibited a late-life decline. This kinetics of RTE decline corresponded closely to the reduction of LN-homing $CCR7^+$ cells and with a transient increase in $CCR7^-S1P1^+$ LN emigrants, but was independent of the decline in export of RTEs from the thymus. The RTE decline in different LNs temporally coincided with a numerical reduction of LN LECs, as well as with a profound disruption of the LN FRC network—early in superficial LNs and late in deep-draining LNs and spleen. Moreover, T cells generated early in life declined numerically in SLOs at around 5 to 6 mo and acquired a virtual memory phenotype. Adoptive transfers of adult T_N cells into old or adult recipients allowed us to map reduced retention of RTEs by LNs at different ages to the age of LNs and not to the intrinsic age of the T_N cells. Finally, functional experiments demonstrated that already at 6 mo, RTEs participated poorly in primary immune responses, particularly at the level of fully differentiated and armed (granzyme B^+, Ag-specific) CD8 T cells. Collectively, these data suggest that LNs do not age equally. Skin-draining LNs exhibited early atrophy and deeper LNs (and spleen) maintained their structure longer, providing a useful temporal framework to dissect the cellular and molecular basis for defects in T_N cell maintenance and function.

Results

Asynchronous Lymph Node Atrophy Dictates Differences in T_N Maintenance between Different Lymph Nodes during Aging. Several studies in both humans and mice have shown the decline in T_N cell numbers during aging (23–25). Using the Rag2-pGFP reporter mouse model we have shown that in the last third of life, even when the thymus is reactivated, RTEs failed to home to and/or be retained well in the old SLOs, particularly the pLNs (14). This may be due to defects in either the old T cells, the pLN microenvironment, or both. Two main experimental approaches have been used to label recent thymic emigrants and study their entry and retention into SLO—direct fluorescein injection into the thymus (26) and genetic marking of recently completed V(D)J recombination by GFP driven by the Rag2 promoter (27). Both are very efficient in short-term labeling of RTEs; however, with both approaches

the label disappears within days due to cell division and protein turnover, and therefore RTEs defined by the expression of RAG-2–driven GFP can be followed, at most, for up to 7 d postthymic exit, and those labeled by fluorescein for even shorter periods.

To stably label and monitor the persistence of RTEs, we used tamoxifen (TAM)-inducible TCRδ^{CreER}.Rosa26-ZsGreen reporter mice (22). These animals were fed a tamoxifen-containing diet for 30 d to induce a wave of ZsGreen-positive RTEs, and the mice were then maintained on normal chow for the next 21 d to allow RTE egress, homing to, and maturation in, SLOs (Fig. 1*A*). Our analysis confirmed that following withdrawal of tamoxifen, ZsGreen labeling of double-positive (DP) thymocytes continued until day 7, but was negligible (<0.1%) by day 14, compared to more than 99% of DP thymocytes labeled during the tamoxifen-diet treatment (*SI Appendix*, Fig. S1*A*). These data confirm the findings in the original publication (22), that developing T cells continue to be labeled for a maximum of 7 d after tamoxifen-diet removal. Therefore, compared to prior studies, RTEs in this manuscript are "older" by up to 4 wk relative to their time of generation in the thymus, which should be considered when comparing data between studies.

We first performed a time-course analysis in a cross-sectional manner to evaluate seeding, maturation, and retention of ZsGreen$^+$ RTEs in different SLOs at 3, 6, 9, 12, 15, 18, 21, and 24 mo of age (*SI Appendix*, Fig. S1*B*). In young animals, nearly a third of all T cells in SLOs were RTEs. That proportion dropped with age. Nonetheless, in agreement with the data from both the Rag2pGFP transgenic mice (21) and older humans (28), we detected both CD4$^+$ and CD8$^+$ RTEs even at 24 mo of age (*SI Appendix*, Fig. S1 *B* and *C*). We found no difference in the ability of RTEs across lifespan to mature (lose the surface expression of CD24 and gain Qa-2) (4) once seeded in different SLOs (*SI Appendix*, Fig. S1*D*). The ratio of RTEs (ZsGreen$^+$) to resident, naive T cells (ZsGreen$^-$, CD44^{lo}62L^{hi}) remained relatively constant across ages, with some variability at 6 and 9 mo and a late decline at 24 mo (*SI Appendix*, Fig. S1*E*). The CD4/CD8 ratio of RTEs produced at different ages also did not change much over lifespan (*SI Appendix*, Fig. S1*F*), consistent with the idea that the late-life increase in CD8 T cells over CD4 T cells is a function of differential peripheral maintenance (21). Moreover, consistent with prior observations from Fink and coworkers (21), we found that the production of ZsGreen$^+$ single-positive cells in the thymus remained constant with age when quantified as a ratio of RTEs to CD4$^+$CD8$^+$ DP thymocytes to control for age-related thymic involution (*SI Appendix*, Fig. S1*G*).

However, major age-related differences were found in the numbers of RTEs detected in different SLOs. Specifically, skin-draining superficial axillary and inguinal LNs exhibited signs of early numerical decline in RTEs around 6 to 9 mo of age, which further progressed with aging (Fig. 1*B*). By contrast, an early decline was not evident in the spleen or brachial LNs, which reside adjacent to the scapula, attached to the biceps muscle, and drain deeper regions of the forearm, shoulder, and neck and not the skin (29, 30). Both the spleen and the brachial LNs only showed significant decline in RTEs around 18 mo (Fig. 1*B* and *SI Appendix*, Fig. S2*A*); a similar late reduction in RTEs was detected in the blood (*SI Appendix*, Fig. S2*A*). This raised a question of whether these observations were a result of differential RTE maintenance/retention or rate of LN atrophy with age. To better understand this, we determined the rate of RTE maintenance or loss in SLOs by analyzing the proportion of ZsGreen$^+$ T cells among the total white blood cells (WBCs). We found that both CD4 and CD8 RTEs exhibited a similar rate of retention or persistence across the different LNs (Fig. 1*C*), with a sharp decline in the rate of RTE retention at 6 mo in all the SLOs, which plateaued thereafter (Fig. 1*C*). Moreover, a similar retention pattern with loss at 6 mo was seen in the spleen, whereas proportions of circulating RTEs increased at 6 mo (*SI Appendix*, Fig. S2*B*). Analysis of WBC numbers in the LNs across ages revealed an asynchronous rate of decline of total cellularity. The skin-draining axillary and inguinal LNs, but not brachial LNs, exhibited overall decline in cellularity (20 to 35% decline compared to 3 mo) as early as 6 mo and never returned back to the numbers seen at 3 mo (Fig. 1*D*). Instead, brachial LNs maintained overall cellularity from 3 to 24 mo. This explains the early decline of absolute RTE numbers in axillary and inguinal LNs compared to brachial LNs, despite a similar rate of RTE retention. Of importance, a significant positive linear correlation between the cellularity of the LN and RTE numbers exists for the axillary and inguinal LNs (*SI Appendix*, Fig. S2*C*), further supporting that age-related atrophy of these LNs might contribute to the reduction in the absolute numbers of RTEs. However, despite maintaining total cellularity (or sometimes increased cellularity) with age, brachial LNs and spleen also accommodated significantly fewer RTEs starting at 6 mo, suggesting constriction of the niche available to receive new RTEs.

The age-dependent decline of RTEs in the SLOs was largely due to the reduction of T_N ZsGreen$^+$ cells (CD62L^{hi}CD44^{lo}) (Fig. 1*E* and *SI Appendix*, Fig. S2*D*), whereas the numbers of central memory (T_{CM}, CD62L^{hi}CD44^{hi}) and effector memory (T_{EM}, CD62L^{lo}CD44^{hi}) ZsGreen$^+$ T cells were very low in all LNs and higher in the spleen (*SI Appendix*, Fig. S1 *H* and *I*). While in the LNs both the CD4$^+$ and CD8$^+$ T_N ZsGreen$^+$ cells showed the same kinetics of decline (early in the superficial and delayed in deeper LNs), we found that splenic (and to a lesser extent, blood) CD4$^+$, but not CD8$^+$, T_N cells showed evidence of an earlier numerical decline (Fig. 1*E* and *SI Appendix*, Fig. S2*D*). RTEs of the T_N phenotype in circulation only showed a significant drop at 21 mo and later (*SI Appendix*, Fig. S2*D*). However, both CD4$^+$ and CD8$^+$ RTEs with a T_N phenotype exhibited a similar rate of retention across ages in different SLOs (Fig. 1*F* and *SI Appendix*, Fig. S2*E*), consistent with the idea that their early numerical decline in axillary and inguinal LNs was largely driven by accelerated LN atrophy (Fig. 1*D*).

Taken together, these results show that 1) the transition from RTE to T_N is unaffected by age; 2) RTE maintenance across SLOs is reduced with aging starting early in life (~6 mo); and 3) early LN atrophy of skin-draining LNs is either a cause, or effect, of reduced RTE and T_N numbers in these LNs. Finally, the asynchronous atrophy of SLOs demonstrates that these changes are not driven by the age-related decline in thymic production but that they instead involve other mechanisms.

Decline of CCR7 Expression and Transient Increases of S1P1 on SLO RTEs Coincide with Age-Related RTE Loss from SLOs. The ability of T cells to reside in the LNs depends on several signals, most notably the expression of the C-C chemokine receptor type 7 (CCR7) and sphingosine 1-phosphate receptor (S1P1) on the surface of RTEs. CCR7 regulates LN homing and retention, and its high-affinity ligands (CCL19 and CCL21) are produced by LN stromal cells, predominantly FRCs, while S1P1 promotes the egress of T cells from the LNs via efferent lymphatics, with LECs producing its ligand,

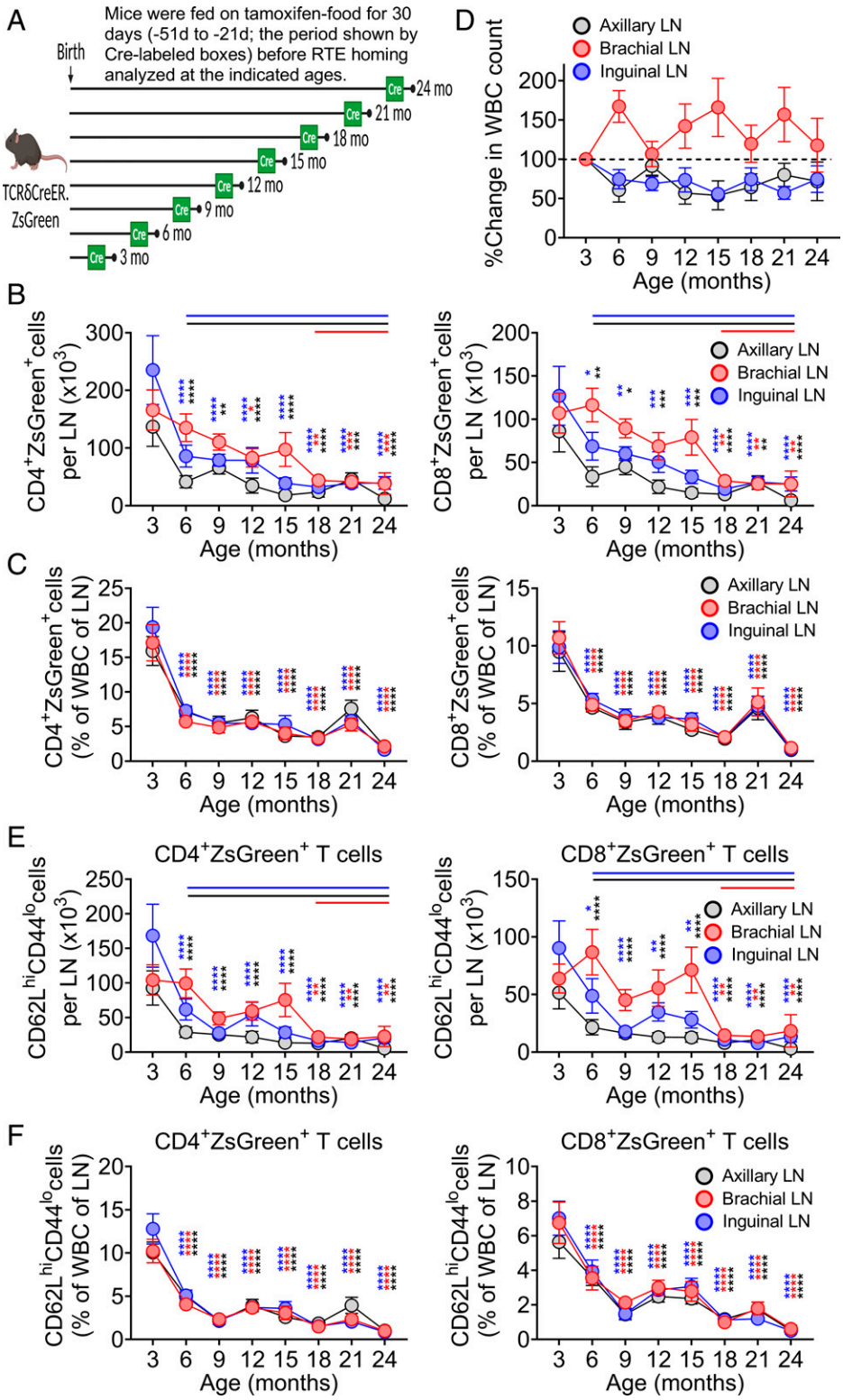

Fig. 1. Differential rate of lymph node atrophy dictates differential number of RTE retention despite similar rate of RTE maintenance. (*A*) Pictorial representation of experimental strategy to label RTEs at different ages, wherein TCRδ^{CreER}.ZsGreen mice were fed on TAM chow for 30 d and revert back to normal chow for another 21 d before analyzing the ZsGreen$^+$ RTEs at indicated timeline ages. Phenotypic analysis of cells from SLOs were performed using multicolor FCM. Data show (*B*) absolute numbers of CD4$^+$ZsGreen$^+$ (*Left*) and CD8$^+$ZsGreen$^+$ (*Right*) T cells and (*C*) percentages of CD4$^+$ZsGreen$^+$ (*Left*) and CD8$^+$ZsGreen$^+$ (*Right*) T cells among the total WBCs in the LNs. (*D*) Percent change in the total WBC count in the LNs across the ages. The cell counts at later ages were normalized to mean absolute count at 3 mo, and percent change was plotted. Data show (*E*) absolute numbers of ZsGreen$^+$CD62L^{hi}CD44^{lo} naive phenotype RTEs among the CD4$^+$ (*Left*) and CD8$^+$ (*Right*) compartments and (*F*) percentages of CD4$^+$ZsGreen$^+$CD62L^{hi}CD44^{lo} (*Left*) and CD8$^+$ZsGreen$^+$CD62L^{hi}CD44^{lo} (*Right*) cells among the total WBC count of pLNs. Data represent pooled results of cross-sectional experiment performed across five to six independent harvests with 9 to 19 mice/age group (*B*–*F*). Error bar represents mean ± SEM (*B* and *C*, *E* and *F*). *$P < 0.05$, **$P < 0.01$, ***$P < 0.001$, ****$P \leq 0.0001$ (P values for different LNs are shown by respective color codes); two-way ANOVA followed by Dunnett's multiple comparison test (multiple comparisons to 3 mo). (*B* and *E*) The horizontal colored lines in the graph denote the time where a significant drop (compared to 3 mo) in the number of RTEs was observed.

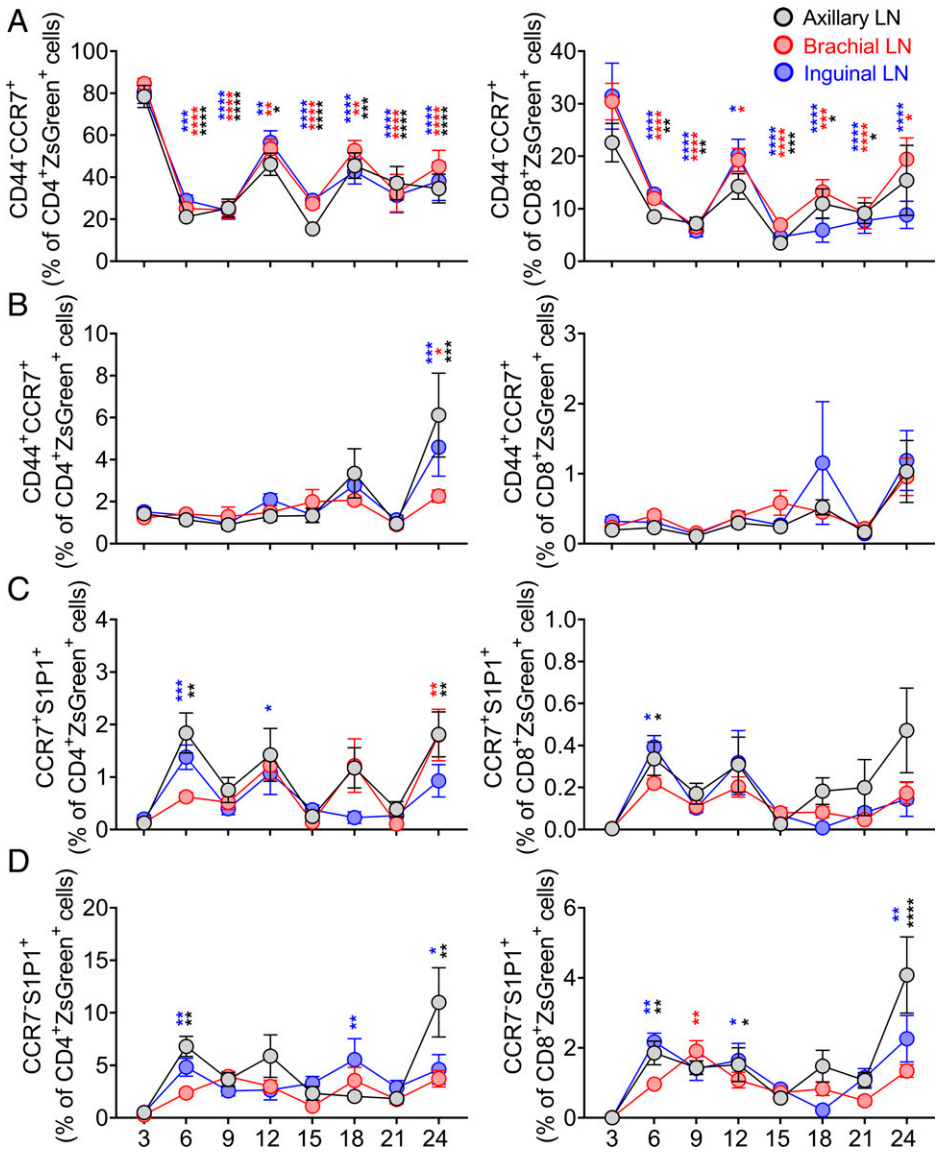

Fig. 2. Decline of CCR7 expression and transient increases of S1P1 are features of RTE retention issue in SLOs during aging. TCRδ^{CreER}.ZsGreen mice were treated as in Fig. 1*A*. Peripheral LNs and spleen and blood cells were stained with CCR7 and S1P1 and analyzed by FCM. (*A* and *B*) Data show frequencies of (*A*) CD44$^-$CCR7$^+$ cells and (*B*) CD44$^+$CCR7$^+$ cells among CD4$^+$ZsGreen$^+$ (*Left*) and CD8$^+$ZsGreen$^+$ (*Right*) T cells in the pLNs. (*C* and *D*) Frequencies of (*C*) CCR7$^+$S1P1$^+$ cells and (*D*) CCR7$^-$S1P1$^+$ cells among CD4$^+$ZsGreen$^+$ (*Left*) and CD8$^+$ZsGreen$^+$ (*Right*) T cells of the pLNs are shown. Data represent pooled results of cross-sectional experiment performed across five to six independent harvests with 9 to 19 mice/age group (*A–D*). Error bars represent mean ± SEM. *$P < 0.05$, **$P < 0.01$, ***$P < 0.001$, ****$P \leq 0.0001$ (*P* values for different LNs are shown by respective color codes used in the figure); two-way ANOVA followed by Dunnett's multiple comparison test (multiple comparisons to 3 mo) (*A–D*).

sphingosine 1-phosphate (31). We examined discrete waves of reporter$^+$ RTEs in SLOs and found that peripheral LNs and spleen had significantly reduced frequencies of CCR7-expressing cells among the reporter$^+$CD44$^-$ naive cells both in CD4$^+$ and CD8$^+$ compartments starting from 6 mo of age (Fig. 2*A* and *SI Appendix*, Fig. S3 *A* and *B*). This decline in CCR7-expressing RTEs was an attribute of SLOs, as we failed to find changes in the circulation (*SI Appendix*, Fig. S3 *A* and *B*). Interestingly, the decreased frequencies of CCR7-expressing RTEs were specifically evident in naive cells but not in T_{CM} cells in SLOs (Fig. 2*B* and *SI Appendix*, Fig. S3 *A* and *C*), suggesting that SLO/LN retention of naive RTEs was selectively affected by aging.

We found that the frequencies of ZsGreen$^+$CCR7$^+$S1P1$^+$ and ZsGreen$^+$CCR7$^-$S1P1$^+$ exhibited a spike at 6 to 9 mo in the SLO, which was more prominent for CD4$^+$ T cells (Fig. 2 *C* and *D* and *SI Appendix*, Fig. S3 *D–F*). Additionally, expression of CCR7 significantly decreased on the surface of CD4$^+$ZsGreen$^+$ and CD8$^+$ZsGreen$^+$ cells as early as 6 mo and was then maintained at this lower level across SLOs thereafter when evaluated as both the frequency of positive cells and mean fluorescent intensity (MFI) of expression (Fig. 2*A* and *SI Appendix*, Fig. S4*C*). In contrast, circulating ZsGreen$^+$ cells exhibited an increased frequency of CCR7$^+$ naive cells and elevated expression levels (by MFI) of CCR7 (*SI Appendix*, Figs. S3*B* and S4*C*). We also noted a transiently increased expression of S1P1 on the surface of CD4$^+$ZsGreen$^+$ and CD8$^+$ZsGreen$^+$ cells at around 9 mo in SLOs and observed expected higher S1P1 levels on their circulating counterparts (*SI Appendix*, Fig. S4 *A*, *B* and *D*). Collectively, reduced representation of CCR7$^+$ and transiently increased representation of S1P1$^+$ cells in the LNs, as well as the increase of circulating ZsGreen$^+$ CD44$^-$CCR7$^+$ and ZsGreen$^+$CD44$^+$CCR7$^+$CD4$^+$ and CD8$^+$ T cells, suggested that the aging LN microenvironment

might not be able to retain these cells, perhaps even facilitating their egress.

Normal Homing and Selectively Reduced Naive Phenotype RTE Retention Characterize LN Aging and Depend on the Age of LNs and Not of T Cells. The decline in T cell maintenance or retention could be due to an age-related intrinsic T cell defect(s), to an age-related change(s) in SLO microenvironment, or both. Given the similar rate of decline in RTE maintenance or persistence in the pLNs, but different kinetics of LN atrophy during aging, we sought to determine whether and which of the SLOs at this age are receptive to incoming RTEs. To test this, we sorted by flow cytometry (FCM) young adult (3 mo) RTEs from tamoxifen-induced TCRδ^{CreER}.TdTomato mice and transferred them into naive adult (3 mo), middle-age (9 mo), and older (19 mo) C57BL/6 mice. Our analysis showed that reporter$^+$ RTE cells homed efficiently into SLOs of all three ages both 1 h and 30 d after transfer (Fig. 3 *A* and *B* and *SI Appendix*, Fig. S5 *A* and *C*), as judged by RTE percentages relative to total WBCs. However, transferred adult RTE numbers were reduced in older recipient LNs compared to younger counterparts, suggesting a possible role of a limited niche available in LNs (empty circle) (Fig. 3*B*). Reporter$^+$ cells homed to, and were well-retained in, spleen at all ages with a significantly larger number of RTEs circulating in the blood of older mice (*SI Appendix*, Fig. S5 *A–D*). Further, we analyzed the phenotypes of the reporter$^+$ cells retained in the SLO 30 d posttransfer and found that LNs and spleen of older age mice had a reduced proportion of naive phenotype reporter$^+$ cells and that reporter$^+$ cells in circulation had a higher frequency of an activated/memory phenotype (Fig. 3*C* and *SI Appendix*, Fig. S5*E*). We conclude that while different older SLOs can all receive RTEs proportional to their overall cellularity, the absolute capacity to receive RTEs and maintain their numbers is reduced with aging.

CD4$^+$ Recent Thymic Emigrants Exhibit Increased Proliferation and Apoptosis in LNs with Aging. Numerical differences in LN RTE cells could simply reflect their immigration and emigration, or could also involve changes in their proliferation and/or survival. To address this issue, we analyzed RTE proliferation by FCM using 5-bromo-2-deoxy-Uridine (BrdU) incorporation and K_i-67 expression, and apoptosis using Annexin-V and live/dead-Zombie Aqua staining. Since we measured a significant decline of RTEs in pLNs at around 9 mo, we analyzed time-stamped cells (generated as in Fig 1*A*) at 3, 9, and 22 to 23 mo of age. Our analysis revealed increased proliferation of RTEs marked by reporter$^+$ (TdTomato) in pLNs of 22- mo-old mice compared to the 3-mo-old adult group, which was particularly pronounced for BrdU$^+$Ki67$^+$ RTEs (*SI Appendix*, Fig. S6 *A* and *B*). These results were statistically significant in all LNs for CD4$^+$ T cells (*SI Appendix*, Fig. S6*B*). Apoptosis was even more dramatically increased in CD4$^+$ RTEs (*SI Appendix*, Fig. S6 *C* and *D*). Importantly, RTE (reporter$^+$) cells in pLNs did not show changes in their proliferation or apoptosis at 9 mo compared to 3 mo (*SI Appendix*, Fig. S6 *A–D*). Neither the hyperproliferation nor increased apoptosis of reporter$^+$ cells was observed in the spleen at examined time points (*SI Appendix*, Fig. S6 *B* and *D*).

Age-Related Changes in the Lymph Node Stromal Compartment Dominantly Impact LEC Numbers and the Integrity of the FRC Reticular Networks. As the maintenance of T_N cells requires homeostatic and survival signals from the LN stromal cells, we next sought to determine whether the numerical decline of T_N cells may correspond to the numerical, structural, and functional changes in LN stromal cells.

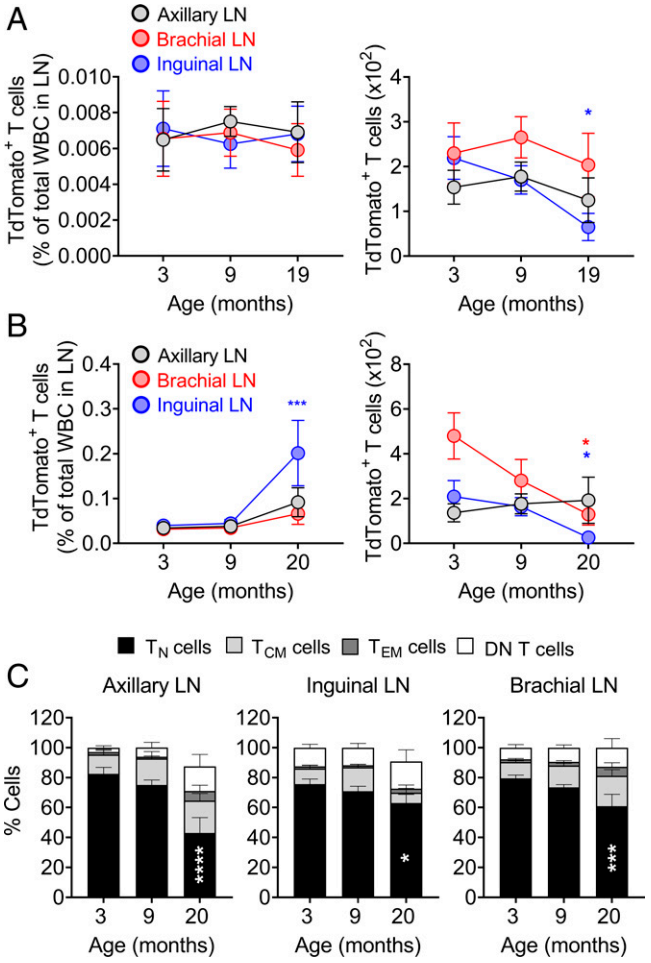

Fig. 3. Normal homing and selectively reduced naive phenotype RTE retention characterize LN aging. TCRδ^{CreER}.TdTomato mice were kept on a tamoxifen-containing diet for 30 d followed by 21 d on the normal chow before TdTomato$^+$ T cells from the spleen and pLNs were FACS sorted at 3 mo of age. About 2 × 10^5 TdTomato$^+$ total T cells were i.v. transferred into 3-, 9-, and 19-mo-old naive C57BL/6 mice. (*A*) One hour later and (*B*) 30 d later, trafficking of transferred cells in the SLOs were analyzed. Data show percentages (*Left*) and absolute numbers (*Right*) of donor TdTomato$^+$ RTEs in the pLNs. (*C*) TdTomato$^+$ T cells from *B* were further analyzed for naive (CD62L^{hi}CD44^{lo}), central memory (CD62L^{hi}CD44^{hi}), effector memory (CD62L^{lo}CD44^{hi}), and DN (CD62L^{lo}CD44^{lo}) phenotypes and percentages of cell populations among TdTomato$^+$ T cells were plotted. Data shown are the pooled result of two independent transfer experiments with n = 8 to 11 recipient mice per group (*A–C*). Data represent mean ± SEM (*A–C*). *P < 0.05, ***P < 0.001, ****$P \leq 0.0001$. One-way ANOVA followed by Tukey's test (*A* and *C*).

Inconsistent results have been reported regarding age-related changes in the number LN stromal cells (5, 14, 17). The disparity may be due to whether the analyses were performed on skin-draining or deeper LNs, the exact enzymatic treatment used for tissue dissociation, subtle differences in the age of animals, or other causes. To exclude technical considerations, we performed FCM analysis and enumeration of the pLN (axillary, inguinal, and brachial) stromal cell subsets following digestion with Liberase TL and DNase-I (17, 20). Our data show that cells from pooled superficial (axillary and inguinal) LNs exhibit a significant reduction of CD45$^-$Ter119$^-$ nonhematopoietic stromal cells at 12 mo of age and thereafter compared to the 6 mo old mice, although they are not reduced relative to the 3-mo time point (Fig. 4 *A* and *B*). The reduction after 6 mo

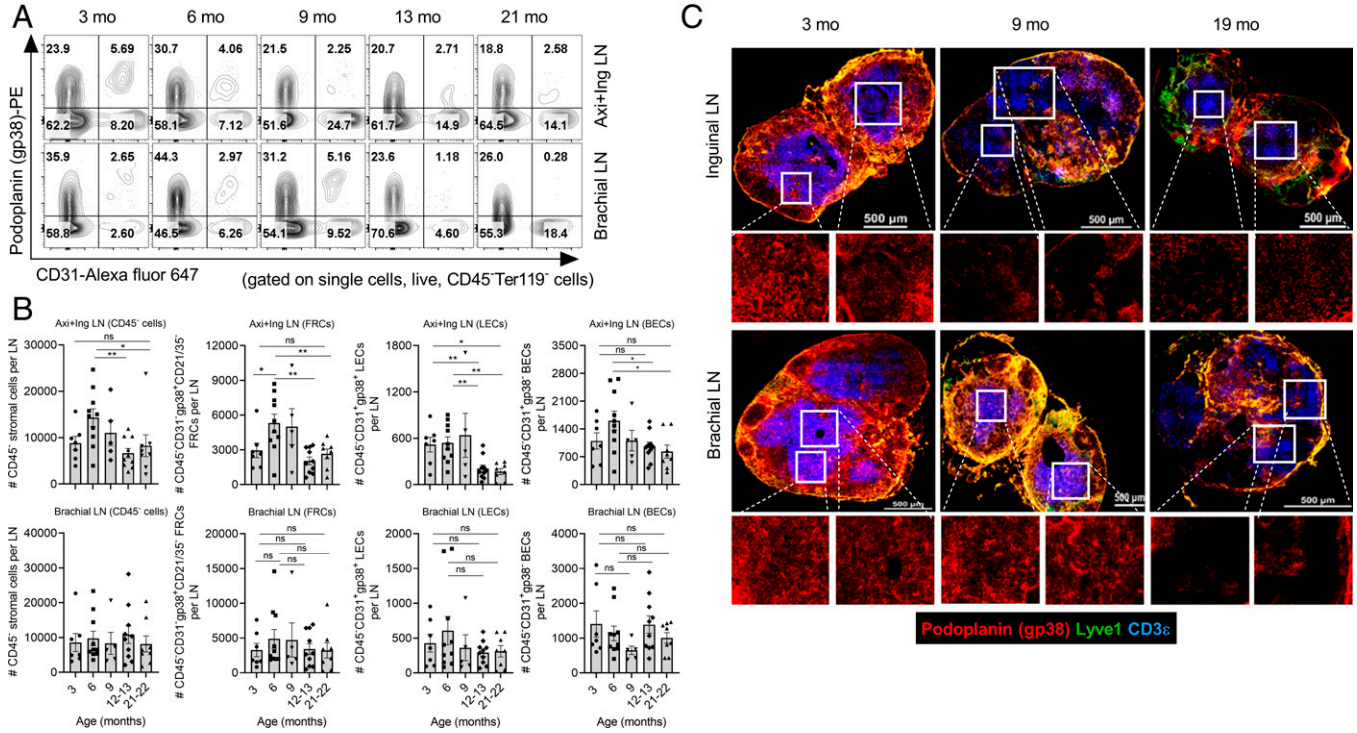

Fig. 4. Timing and effect of T_N cell numerical decline on the lymph node stromal compartment during aging. One side of peripheral LNs of the naive wild-type C57BL/6 mice of indicated timeline ages were processed for lymphocyte analysis and contralateral ones were digested with Liberase TL and DNase-I for stromal cell analysis. (*A*) Representative FACS plots show staining of podoplanin (gp38) and CD31 on stromal cells gated on single cells, live, and $CD45^-Terr119^-$ cells. The number in the quadrant indicates frequencies of the indicated cell populations. (*B*) Data show absolute numbers of $CD45^-$ total stromal cells, FRCs ($CD45^-CD31^-gp38^+CD21^-CD35^-$), LECs ($CD45^-CD31^+gp38^+$), and BECs ($CD45^-CD31^+gp38^-$) of the pool of axillary and inguinal (Axi+Ing) LNs (*Top*) and brachial LNs (*Bottom*). Each dot represents individual mouse and data represent mean ± SEM, $n = 5$ to 10 mice/group. $^*P < 0.05$, $^{**}P < 0.01$; ns, nonsignificant; one-way ANOVA followed by Dunnett's multiple comparison test. (*C*) Representative images of 8 μ-thick cryosections of the LNs stained with Lyve-1 (green), podoplanin (gp38; red), and CD3 (blue) are shown. The zoomed images of the region marked with white squares are shown at the *Bottom* of the respective images. Images are representative of five mice/group. Magnification, 60×. (Scale bar, 500 μm.)

was consistent with the pattern of T_N cell decline. Furthermore, FRCs ($CD45^-Ter119^-CD31^-gp38^+CD21^-CD35^-$), LECs ($CD45^-Ter119^-CD31^+gp38^+$), and BECs ($CD45^-Ter119^-CD31^+gp38^-$) followed a similar trend of a numerical decline in the axillary and inguinal LNs (Fig. 4*B*), with the most pronounced changes in the numbers of LECs. In contrast, the stromal cells in the brachial LNs appeared unchanged (Fig. 4*B*). To evaluate another deep tissue-draining LN, we tested iliac LNs that drain the prostate and reproductive organs and the lateral tail. We did not find fluctuations in the stromal cell numbers of the iliac LNs at any of the ages analyzed (*SI Appendix*, Fig. S7*A*).

To interrogate whether the LN stromal networks undergo structural or organizational alterations, we used confocal microscopy on frozen LN sections at 3, 9, and 19 mo of age. Our image analysis showed that inguinal LNs exhibit gross structural alterations in podoplanin (gp38) staining at 9 and 19 mo, suggesting FRC network disruption at these ages (Fig. 4*C*, high magnification *Insets*). In parallel, we noted fewer $CD3^+$ T cells confined to the characteristic T cell zones at 9 mo, which were further reduced at 19 mo. A similar FRC network disruption was observed at 19 mo in brachial LNs, whereas their stromal integrity was well maintained at 9 mo (Fig. 4*C*). We next assessed whether FRC network alterations may correlate with the levels of soluble mediators produced by FRCs, including the survival factor IL-7 and chemokines CCL19 and CCL21. The IL-7 and CCL21 expression did not change in old LNs compared to adult (*SI Appendix*, Fig. S7*B*). Old LNs seemed to have more CCL19 compared to adult; however, group means did not reach statistical significance (*SI Appendix*, Fig. S7*B*). Interestingly, CCL19 levels tended to increase wherever the FRC network was perturbed, i.e., at 9 mo in inguinal nodes and 18 mo in brachial nodes (*SI Appendix*, Fig. S7*B*). Collectively, this shows that despite unchanged numbers of FRCs at 9 mo, inguinal LNs start exhibiting gross FRC network alterations and similar changes occur in the brachial LNs at 19 mo, paralleling their reduced receptiveness for RTEs (Fig. 1 *B* and *C*). As this also correlates with the increase in CCL19 in respective LNs, it may be compensatory in nature.

Life-Long Changes in Homeostatic Maintenance and Phenotype of T Cells Generated in Early Life. How long and how well are T_N cells generated in youth maintained in SLOs throughout their life? To better understand this, we used $TCR\delta^{CreER}$.TdTomato mice, induced by a tamoxifen diet for 30 d at 2 mo of age, generating a wave of RTEs marked for life (Fig. 5*A*). Tracking time-stamped cells allowed us to longitudinally monitor and analyze T cells generated at 2 mo, across the life of a mouse. Time-stamped cells generated at 2 to 3 mo started to decline as early as 5 to 6 mo of age in the SLOs, followed by further, more gradual, decline from 6 to 24 mo (Fig. 5*B* and *SI Appendix*, Fig. S8*A*). Notably, all SLOs showed similar pattern of decline for both $CD4^+$ and $CD8^+$ time-stamped cells. In the blood, the decline was evident from 12 mo of age (*SI Appendix*, Fig. S8*A*). Again, the decline in the overall numbers of cells "born" in youth was driven by a significant decline of T_N cells (Fig. 5*C* and *SI Appendix*, Fig. S8*B*). Collectively, these results suggest that aging SLOs, and particularly pLNs, exhibit an early defect in the maintenance of T cells.

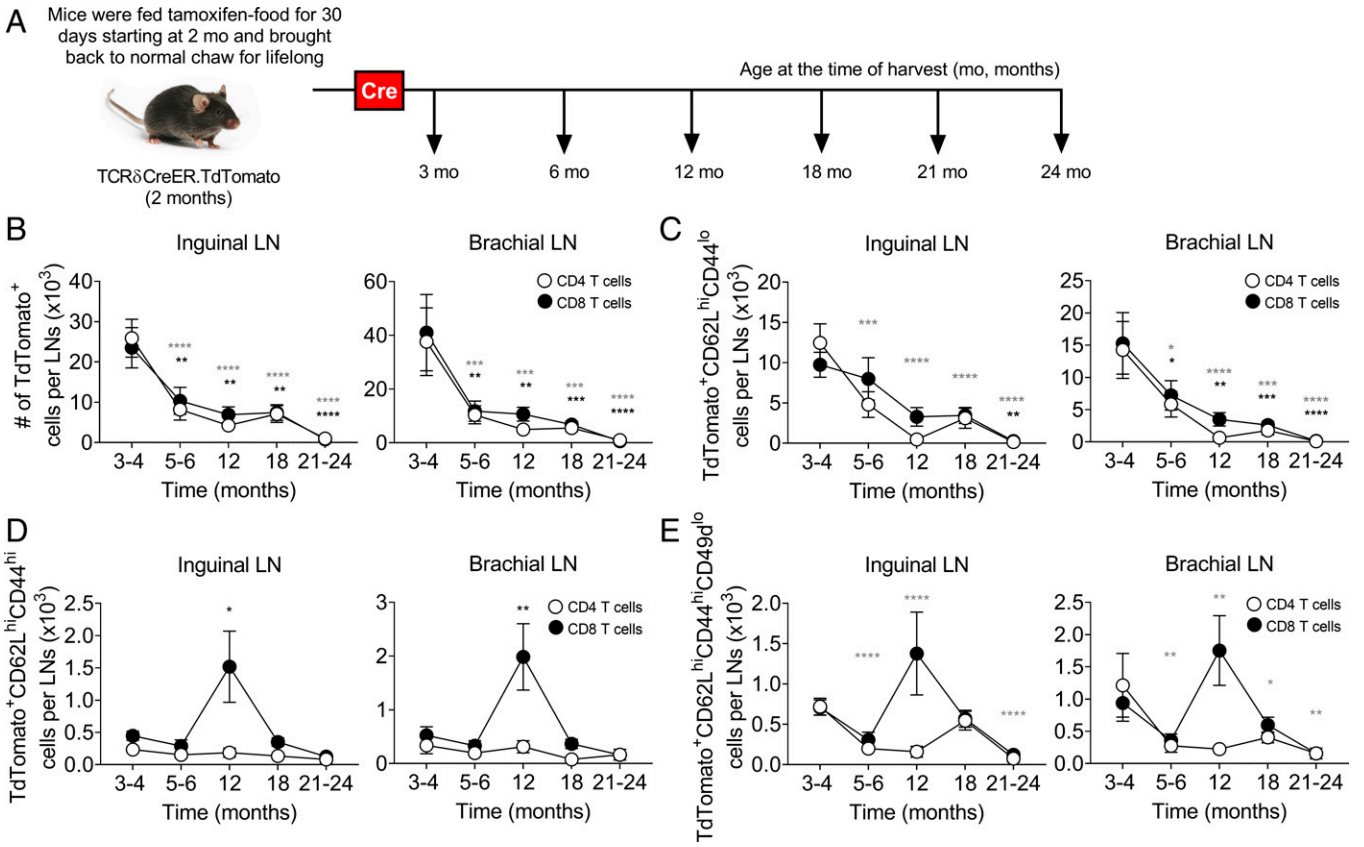

Fig. 5. SLO microenvironment failed to maintain T cells generated in early life during aging under steady-state condition. (*A*) Pictorial representation of experimental strategy to label T cells generated (time-stamped cells) at 2 to 3 mo of age (time where Cre-expressed), wherein TCRδ^{CreER}.TdTomato mice were fed on TAM chow for 30 d starting at 2 mo of age and thereafter lifelong maintained on normal chow before analyzing the TdTomato$^+$ time-stamped cells by FCM at indicated timeline ages under homeostatic condition. (*B–E*) Absolute numbers of (*B*) total TdTomato$^+$ time-stamped cells and (*C*) TdTomato$^+$ time-stamped cells with naive (CD62L^{hi}CD44^{lo}), (*D*) central memory (CD62L^{hi}CD44^{hi}), and (*E*) virtual memory (CD62L^{hi}CD44^{hi}CD49d^{lo}) phenotype in the inguinal and brachial LNs, spleen, and circulation are shown. Data represent pooled results of a longitudinal experiment performed across five independent harvests with 11 to 18 mice/age group (*A–E*). Error bar represents mean ± SEM. *$P < 0.05$, **$P < 0.01$, ***$P < 0.001$, ****$P \leq 0.0001$ (P values for CD4$^+$ and CD8$^+$ T cells are denoted by gray and black stars, respectively); one-way ANOVA followed by Dunnett's multiple comparison test (compared to 3 to 4 mo) (*B–E*).

Some of the CD8$^+$ time-stamped cells acquired the T_{CM} (CD62L^{hi}CD44^{hi}) phenotype, and we detected their spike (a 2- to 3-fold increase in numbers) at 12 mo and 12 to 18 mo in SLOs and the circulation, respectively, after which they returned to baseline at older ages (Fig. 5*D* and *SI Appendix*, Fig. S8*C*). While some of the T_N cells differentiate into T_{EM} and T_{CM} cells as a consequence of antigen stimulation, there is also a pool of T_N cells that differentiate into a T_{CM}-like phenotype without exposure to manifest microbial infection (32), likely due to adaptation to reduced homeostatic signals, and the accumulation of these antigen-independent virtual memory T (T_{VM}) cells is one of the hallmarks of aging in specific pathogen-free laboratory mice (33–37). We found that most of the accumulated time-stamped CD8$^+$ T_{CM} cells were of the virtual memory phenotype (CD62L^{hi}CD44^{hi}CD49d^{lo}) around 12 mo of age in the pLNs (Fig. 5*E* and *SI Appendix*, Fig. S8*D*). Moreover, CD8$^+$ T_{VM} cells accumulated in circulation, but not in the spleen (*SI Appendix*, Fig. S8*D*). By contrast, CD62L^{hi}CD44^{hi}CD49d^{hi} true-central memory T (T_{CM}) cells were not detectable in pLNs or blood, and did not increase at 12 mo in any of the organs examined (*SI Appendix*, Fig. S8*E*).

We conclude that following the initial drop in maintenance of T_N cells at an early age, there is a transient wave of conversion of T_N cells into T_{VM} cells that is likely compensatory in nature, whereby, presumably, these cells might shift their maintenance pattern from IL-7 to IL-15, consistent with our prior data (34). In line with this, we observed the increased accumulation of these T_{VM} cells in the bone marrow, a rich source of IL-15, between 6 mo and 18 mo (*SI Appendix*, Fig. S8*F*).

Participation of RTEs in a Skin-Initiated Immune Response Declines at an Early Age. Given the surprisingly early changes in superficial LNs and in SLOs overall, we sought to examine to what extent newly generated T cells (RTEs) can participate in an immune response. We challenged tamoxifen-induced TCRδ^{CreER}.ZsGreen or TCRδ^{CreER}.TdTomato mice with footpad injection of RepliVAX-WN (R-WN), a single-cycle WNV vaccine lacking the viral capsid (C) protein, and thus unable to package new virions (38). R-WN carries the main WNV antigens immunodominant in B6 mice and confers protection against subsequent lethal WNV challenge in both adult and old mice (39). However, in old mice, primary R-WN immunization induces significantly reduced antigen-specific T and B cell responses. We analyzed responses of reporter$^+$ cells to WNV-immunodominant NS4b$_{2488}$ CD8$^+$ epitopes in the blood using the NS4b$_{2488}$:Db tetramers (39, 40) and found robust responses at 3 mo of age by percentage and absolute number of tetramer$^+$ cells and differentiation of CD8$^+$ cells into cytotoxic granzyme B (GzB)$^+$ effectors (Fig. 6 *A–D*). However, at 7 to 8 mo, the response was already dramatically blunted, to the point that the circulating NS4b$_{2488}$:Db tetramer$^+$reporter$^+$ cells with a cytotoxic (GzB$^+$) phenotype were barely detectable in the blood (Fig. 6*D*). We also examined recall responses in the

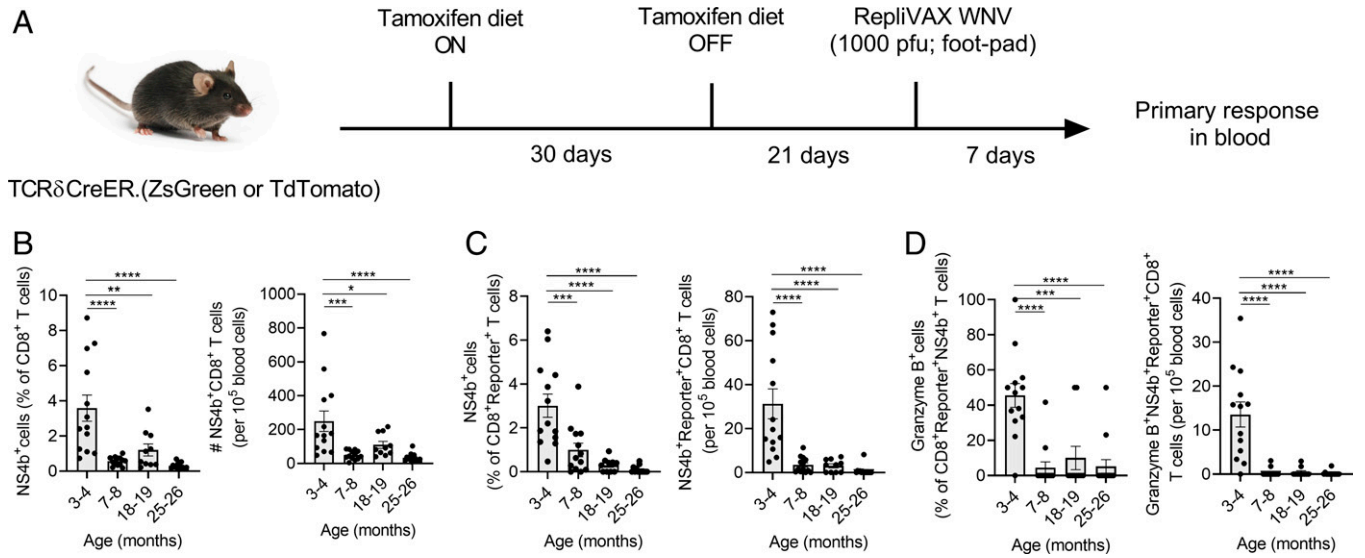

Fig. 6. RTEs responsive to the Replivax West Nile virus vaccine decline at the age where SLOs show defects in RTE maintenance. (*A*) TCRδ^{CreER}.ZsGreen and TCRδ^{CreER}.TdTomato mice were fed on tamoxifen-containing diet for 30 d and subsequently maintained on normal diet for the next 21 d. At day 21, mice were s.c. injected into the foot pad with Replivax West Nile virus vaccine (1×10^3 pfu). After 7 d postinjection, blood was collected and West Nile virus–specific CD8$^+$NS4b$^+$ T cells in the total and reporter (ZsGreen$^+$ or TdTomato$^+$) T cells were analyzed. (*B*) Data show percentages of NS4b$^+$ T cells among the CD8$^+$ T cells (*Left*) and numbers of circulating NS4b$^+$CD8$^+$ T cells (*Right*). (*C*) Data show percentages of NS4b$^+$ cells among the CD8$^+$reporter$^+$ T cells (*Left*) and numbers of circulating NS4b$^+$reporter$^+$CD8$^+$ T cells (*Right*). (*D*) Data show percentage of granzyme B$^+$ cells among CD8$^+$reporter$^+$NS4b$^+$ T cells (*Left*) and numbers of circulating granzyme B$^+$NS4b$^+$reporter$^+$CD8$^+$ T cells (*Right*). (Data represent pooled results from three independent experiments with 10 to 14 mice per age group (*B–D*). Each circle represents individual mice. Error bar represents mean ± SEM. *$P < 0.05$, **$P < 0.01$, ***$P < 0.001$, ****$P \leq 0.0001$; one-way ANOVA followed by Tukey's multiple comparison test (*B–D*).

same animals and found that consistent with our prior data (39), recall stimulation produces strong responses even in the oldest previously vaccinated animals (*SI Appendix*, Fig. S9 *A* and *B*) at the level of overall CD8$^+$ T cell response, particularly in the spleen. Responses by CD8 RTEs generated at different ages (time-stamped, reporter$^+$ cells) (*SI Appendix*, Fig. S9 *C* and *D*) were also more numerous and robust and showed a more gradual pattern of decline, which was particularly evident for the CD8$^+$reporter$^+$GzB$^+$ effector cells in the spleen between 3 and 24 mo (*SI Appendix*, Fig. S9*D*).

Collectively, these results suggest that RTEs participate in primary immune responses to subcutaneous/intradermal vaccination at a young age but that primary responses are barely detectable as early as 6 to 8 mo, although they could be expanded by recall stimulation, in which case they wane only later in life. The implications of these findings for immunity and vaccination are discussed below.

Discussion

Homeostasis of T_N cells is maintained by a critical balance between new T cell (RTEs) production and entry into SLOs and the turnover (loss) of mature T_N cells due to antigenic stimulation (phenotypic conversion into memory cells) or impaired maintenance in the SLOs (death or conversion into virtual memory cells) (21). The numerical loss of T_N cell numbers is the most reliable measure of immune aging and is due to the combined effects of an early-life thymic involution that curtails new T_N production and a late-life dysregulation of their homeostatic maintenance in secondary lymphoid organs (41). The main unexpected finding of this study is that despite a similar rate of RTE loss in all SLOs, superficial skin-draining LNs exhibit early (6 to 9 mo) atrophy and numerical decline of RTEs, while spleen and deeper brachial (and in limited experiments, iliac) LNs maintain RTE numbers until later in life (18 mo and older). This defect (or RTE loss) corresponded closely to the reduction of LN-homing CCR7$^+$ cells and a transient increase in CCR7$^-$S1P1$^+$ LN emigrants, and to the age-related structural deterioration of the LN FRC network. Further, T cells generated in early life started declining in SLOs at 6 mo and showed signs of phenotypic change toward virtual memory–like phenotype. Finally, functional participation of RTEs in cutaneous priming responses also fell precipitously around 6 to 8 mo, as measured by effector responses of time-stamped CD4$^+$ and CD8$^+$ cells against RepliVAX-WNV vaccination.

To integrate these results into a plausible model of lifespan-related events, one needs to consider several points. Previous reports have clearly shown that maximal thymic output in mice occurs by 6 to 7 wk of life (21, 42). However, the data presented here cannot be explained by a mere decline in thymic output because we find that time-stamped RTEs in the same mouse at 6 to 9 mo fail to inhabit axillary and inguinal LNs, but not brachial LNs and spleen, and that the same cells are replete in the blood at the same time points. This suggested that seeding and/or retention of RTEs in superficial SLOs may exhibit early defects with aging. Transfer experiments confirmed that early seeding (1 h) was not different across SLOs, and we found that maturation of RTEs into the Qa2^{hi}CD24^{lo} phenotype (43, 44) was uniform as well. We therefore hypothesized that RTE/T_N retention is asynchronous across SLOs over the lifespan.

In support of this hypothesis, we found that the inguinal and axillary LNs exhibit early life (starting at 6 mo) atrophy, losing total WBCs that constitute about 99% of LN cells. This early life atrophy might also contribute to the reduction of the niche size available to harbor ZsGreen$^+$ RTEs, because despite the fact that the loss of RTEs similarly affected all LNs, the absolute numbers of RTEs significantly decline specifically in inguinal and axillary LNs. Moreover, decreasing size (as measured by proxy of change in total WBC numbers) of the involuting LNs correlated well with the decline in RTE numbers

specifically in axillary and inguinal LNs, suggesting that due to the lack of space/niche availability, RTEs tend to exit from these LNs and circulate elsewhere. Consistent with this, among the RTEs found in the SLOs, the frequencies of CCR7-expressing cells started declining as early as 6 mo. CCR7 is a key chemokine receptor needed to guide lymphocytes to the SLO in response to CCL19 and CCL21 gradient. These chemokines are produced by lymphoid stromal cells, particularly FRCs and LECs (45, 46). Time-stamped RTEs also showed an (transient) increase in S1P1 at 6 mo in the early-involuting SLOs and a more continuous presence of these cells in the brachial LNs and spleen, suggesting that these cells exhibit a SLO-emigrating phenotype, whereby the transient increase in the level of S1P1 might be enough to overcome the reduced CCR7-mediated retention signal strength (47). We further found an increase in $CCR7^+$ RTEs (of both the $S1P1^-$ and $S1P1^+$ phenotypes) in the circulation at the respective ages. Finally, analysis of time-stamped cells generated early in life (between 1.5 and 3 mo) showed that an early decline in T_N retention across SLOs was followed by a transient wave of antigen-independent T_{VM} cells, consistent with the conversion of $T_N > T_{VM}$ cells with aging, which then moved from the LNs to the bone marrow.

Prior work reported variable changes in SLO stromata with aging, with some authors reporting reduced stromal cell numbers (5, 48), and others not (17), but all agreeing on some extent on the disorganization of FRC networks in old mice. To address these discrepancies, and correct for the influence of different enzymatic digestion protocols, we have used the procedure of Masters et al. (17) to reevaluate this in SLOs across age and anatomic locations. While the brachial LNs exhibited stable numbers of $CD45^-$ stromata, FRCs, LECs, and BECs across aging, the early-involuting superficial LNs (axillary and inguinal) maintained the numbers of total $CD45^-$ stromal cells and of FRCs and LECs until 9 mo and then experienced a significant decline in all three populations from 12 mo on. Structural analysis of SLO stroma organization revealed that a numerically unperturbed stromal compartment does not equate normal structure of stromal networks. Specifically, while the inguinal LNs at 9 mo and brachial LNs at 19 mo each contained comparable FRC and LEC numbers, they each exhibited a striking defect in the FRC (podoplanin/$gp38^+Lyve1^-$ cells in the images) network that was markedly less dense at sites corresponding to T cell zones. This discordant deterioration of the superficial LN FRC network could be expected to lead to inefficient access of T_N cells to chemotactic and maintenance factors, including IL-7, and most likely is responsible for reduced niche availability to receive RTEs. We believe that in this case FRC disorganization impairs access to trophic factors, rather than their levels, because we found that with aging, levels of IL-7, CCL19, and CCL21 were not reduced compared to 3-mo-old mice, consistent with prior data (5, 14), and in fact we found evidence for a potential compensatory increase at 9 mo for IL-7 and CCL19.

Based on all of the above, we can integrate the data into a hypothetical model based on the putative cross-talk between lymphocytes and stromal cells in SLOs (Fig. S10). Step 1 would occur as the initial reduction of RTE/T_N from the thymus leads to less trafficking of these cells to the SLOs, somewhere around 3 to 5 mo of life in murine superficial SLOs. This will result in an initial, but subtle, insult/injury to the SLO stromal cells, perhaps in the form of reduced trophic signals to FRCs/LECs. Step 2 would ensue when FRCs/LECs react to this reduction by reduced metabolic or functional fitness and FRCs potentially begin to retract their processes and thereby begin to reduce the density of the FRC network. This will result in reduced survival/trophic signaling to the surrounding T_N cells, and in an overall reduction in the RTE niche size, facilitating the loss of T_N cells (step 3), and the entire sequence will progress as a feed-forward negative loop, leading to increased SLO stromal dysregulation and progressive reduction in RTE/T_N maintenance. Consequences of this loop are evident as reduced RTE/T_N retention, disrupted FRC networks, changes in RTE/T_N homing receptor expression toward emigrating phenotype, and subsequently toward virtual memory fate and alternative maintenance. At older ages, we found that this can even take a form of increased proliferation, and, in the case of $CD4^+$ T cells, also increased apoptosis, previously described in the literature (21, 49). It remains to be determined whether $CD4^+$ T_N cells in old LNs are experiencing proliferation-induced apoptosis or may be attempting to compensate for increased apoptosis by increasing the rate of proliferation.

The above model remains to be experimentally tested in greater detail, particularly on the mechanistic side. In that context, any model will have to account for the finding that superficial, but not deeper, LNs are susceptible to early atrophy. Work on that question is currently in progress. One could speculate that different amounts of antigen exposure of the LNs at different anatomic locations might be a potential factor; however, at the present, it is not possible to exclude roles of age-related low-grade inflammation and/or increased oxidative or other stress to superficial LNs. Causal association of such mechanisms with the structural alterations of the LN organization and integrity will be key to establish whether an altered FRC network in inguinal LNs is the cause or consequence of early age–related atrophy. Regardless of the mechanisms, however, we have shown that the end result of all of the above changes is a drastic compromise of cutaneous immunity to the point that already at 6 to 8 mo of age (an equivalent to early middle age in humans), superficial LNs, and the cells therein practically fail to mount any meaningful effector T cell response in laboratory-specific pathogen-free mice. Mice mature to adulthood between 3 and 6 mo of age, 3 to 6 mo B6 mice are considered equivalent to a 20- to 30-y-old person (50). Based on our data, where LNs in mice younger than 6 mo undergo minimal LN atrophy, and that the rate increases at and over the age of 6 mo, we would suggest that 4 to 6 mo of age in B6 mice may be an appropriate age for measuring immune responses comparable to a young adult human. Of interest, this corresponds very well to the accepted guidelines of mouse ages for gerontological research (51). Investigation of older mice, at 12 and 24 mo of age, would be recommended to extend applicability of preclinical vaccine trials to most of the human population.

Intramuscular injection into the deltoid muscle is the most common route for adult vaccination in humans. Our data mandate careful and direct comparison of the magnitude of vaccine responses depending on route of immunization at different ages, which in turn should determine whether targeting certain LNs could improve vaccine responses in older adults. Similarly, this type of data would inform whether efficacy of immunomodulatory as well as cancer immunotherapies may be improved by different routes of delivery depending on SLO targeting. Practical considerations here will need to be further formally investigated as related to older humans, but these findings certainly correspond very well to clinical observations that older adults rarely, if ever, react to acute infection with subcutaneous lymphadenopathy (18, 52, 53).

Materials and Methods

Mice. Wild-type C57BL/6 mice of varying ages were obtained from the National Institute of Aging's breeding colony. The B6.129S-Tcrd$^{tm1.1(cre/ERT2)Zhu}$/J (TCRδ^{CreER}) strain was generously provided by Yuan Zhuang, Duke University, Durham, NC. B6.Cg-*Gt(ROSA)26Sor*$^{tm6(CAG-ZsGreen1)Hze}$/J (Rosa26.ZsGreen) and B6.Cg-*Gt(ROSA)26Sor*$^{tm14(CAG-TdTomato)Hze}$/J (Rosa26.TdTomato) mice were purchased from The Jackson Laboratory. TCRδ^{CreER} mice were bred either with Rosa26.ZsGreen or Rosa26.TdTomato to generate TCRδ^{CreER}.ZsGreen and TCRδ^{CreER}. TdTomato reporter strains that label RTEs green and red, respectively. All mice strains were maintained under specific pathogen-free conditions at the university animal care facility, University of Arizona, Tucson, AZ. All experiments were performed in compliance with the guidelines of the University of Arizona's Institutional Animal Care and Use Committee.

Mice Treatment. TCRδ^{CreER}.ZsGreen mice were fed TAM-containing chow for 30 d followed by normal chow for the next 21 d before they were euthanized to analyzed RTEs at 3, 6, 9, 12, 15, 18, 21, and 24 mo of age. For adoptive transfer, life-long maintenance of RTEs generated at early life, and some of the immunization experiments, we used TCRδ^{CreER}.TdTomato mice, where similar to ZsGreen labeling, RTEs were labeled with TdTomato reporter. To generate RTEs in early life, TCRδ^{CreER}.TdTomato mice at 2 mo of age were fed on TAM chow for 30 d followed by lifelong maintenance on normal chow.

Lymph Node Stromal Cell Isolation and Analysis. For simultaneous analysis of stromal cells and lymphocytes, the left side of the axillary, inguinal, and brachial LNs were processed for stromal cell analysis, and the right side was used for lymphocyte enumeration. We chose to study the brachial LNs for two reasons: First, the lymphatics of the brachial LNs are not connected to those of the axillary and inguinal LNs (29, 30). Second, brachial LNs drain the deltoid muscle, which is the preferred site for most vaccine injections and are therefore biologically interesting from the standpoint of understanding how T_N cell homeostasis may influence vaccine responses. While we confirmed some results in deeper-draining illiac LNs, we did not systematically pursue them, as they also share lymphatic circulation with inguinal LNs. See *SI Appendix, SI Methods* for details.

Flow Cytometry. Cells were harvested from the peripheral lymph nodes, thymus, and spleen via mechanical disassociation through a 40-μm cell strainer using a syringe plunger. Spleen cells and blood were treated with ammonium–chloride–potassium lysis buffer to lyse red blood cells (RBCs). About 1 to 2 $\times$ 10^6 cells were stained with fluorescence-conjugated antibodies (*SI Appendix*, Table 1) and acquired on an LSR Fortessa (BD Biosciences). For details, see *SI Appendix, SI Methods*.

Immunohistochemical Staining of Lymph Nodes. Mice were euthanized via isoflurane overdose, peripheral LNs were harvested, and immediately snap frozen in optimal cutting temperature medium (Sakura Finetek). The 8- to 10-μm cryosections were prepared and fixed in chilled acetone for 5 min, air dried, washed with phosphate-buffered saline, and stained. For details, see *SI Appendix, SI Methods*.

In Vivo Homing of RTEs to Secondary Lymphoid Organs. TCRδ^{CreER}.ZsGreen and TCRδ^{CreER}.TdTomato mice were fed with TAM chow for 30 d followed by normal chow for 21 d before mice were euthanized at 3 mo of age. Spleen and pLNs were harvested, single-cell suspensions prepared, and total T cells were enriched using the mouse CD3ε Microbead kit (Miltenyi Biotec), according to the manufacturer's instructions. RTEs (ZsGreen$^+$ or TdTomato$^+$) were fluorescence-activated cytometry sorted (FACS) (purity >95%), and a total of 2 $\times$ 10^5 cells were i.v. transferred into 3-mo, 9-mo, and 19- to 20-mo-old C56BL/6 mice via a retroorbital route. The homing or retention of reporter-positive RTEs in the SLOs was analyzed by flow cytometry after 1 h and 30 d posttransfer.

Analysis of RTE Responses to West Nile Vaccination. TCRδ^{CreER}.TdTomato or TCRδ^{CreER}.ZsGreen mice were fed on a tamoxifen-containing diet for 30 d and subsequently maintained on a normal diet for the next 21 d. At day 21, mice were subcutaneously (s.c.) injected in the hind foot pad with Replivax West Nile virus vaccine (1 $\times$ 10^3 pfu). At day 7 postinjection, mice were bled retroorbitally, and primary responses to vaccination were assessed using FCM analysis of WNV-immunodominant NS4b$_{2488}$ CD8$^+$ epitope using the NS4b$_{2488}$:Db tetramer. Mice further received a booster dose of Replivax West Nile virus vaccine (1 $\times$ 10^3 pfu) at day 45 after primary immunization, and recall responses of total and reporter-positive NS4b$^+$CD8$^+$ T cells were analyzed in the SLO.

Statistical Analysis. Data for RTE numbers were collected over multiple timeline experiments with overlapping age groups and pooled together. Data are expressed as the mean $\pm$ SEM. As indicated in the figure legends, statistical analysis was performed by one-way or two-way analysis of variance (ANOVA) followed by Dunnet's multiple comparison test and a Mann–Whitney *U* test using Prism 8 software. Comparisons of the group mean differences were considered significant at $P < 0.05$.

Detailed methods can be found in *SI Appendix*.

Data Availability. All study data are included in the article and/or *SI Appendix*.

ACKNOWLEDGMENTS. We thank Dr. Y. Zhuang (Duke University) for generously providing us TCRδCre.ER mice. We thank Mr. Jose L. Padilla-Torres, and the university animal care facility, (University of Arizona, Tucson, AZ) for maintaining mouse colonies. We are grateful to the University of Arizona/University of Arizona Cancer Center (UACC) Shared Flow Cytometry Resource and the Imaging Core Facility, supported by the UACC Support Grant P30 CA023074 for technical help with flow cytometry and microscopy. We thank Dr. Laura Hale (the Duke Human Vaccine Institute, Duke University, Durham, NC); Dr. Nancy R. Manley (Department of Genetics, University of Georgia, Athens, GA); Dr. Ellen R. Richie (MD Anderson Cancer Center, Austin, TX); and Dr. Lauren I. R. Ehrlich (Department of Molecular Biosciences, Institute of Cellular and Molecular Biology, University of Texas at Austin, Austin, TX) for scientific discussion, critical reading of manuscript, and other input. This work is supported in part by US Public Health Service Awards AG052359 and AG020719 and the Bowman Endowed Professorship in Medical Sciences (J.N.-Ž.). Work performed at Duke University was in the Duke Regional Biocontainment Laboratory, which received partial support for construction from NIH/National Institute of Allergy and Infectious Diseases (AI058607 to G.D.S.).

Author affiliations: [a]Department of Immunobiology, University of Arizona College of Medicine-Tucson, Tucson, AZ 85724; [b]Arizona Center on Aging, University of Arizona College of Medicine-Tucson, Tucson, AZ 85724; [c]Duke Human Vaccine Institute, Duke University, Durham, NC 27710; [d]Program in Immunology, Fred Hutchinson Cancer Center, Department of Immunology, University of Washington, Seattle, WA 98109; [e]Department of Immunology, Memorial Sloan-Kettering Cancer Center, New York, NY 10021; and [f]BIO5 Institute, University of Arizona, Tucson, AZ 85719

1. S. P. Berzins, R. L. Boyd, J. F. Miller, The role of the thymus and recent thymic migrants in the maintenance of the adult peripheral lymphocyte pool. *J. Exp. Med.* **187**, 1839–1848 (1998).
2. P. J. Fink, The biology of recent thymic emigrants. *Annu. Rev. Immunol.* **31**, 31–50 (2013).
3. A. M. Berkley, P. J. Fink, Cutting edge: CD8+ recent thymic emigrants exhibit increased responses to low-affinity ligands and improved access to peripheral sites of inflammation. *J. Immunol.* **193**, 3262–3266 (2014).
4. T. E. Boursalian, J. Golob, D. M. Soper, C. J. Cooper, P. J. Fink, Continued maturation of thymic emigrants in the periphery. *Nat. Immunol.* **5**, 418–425 (2004).
5. B. R. Becklund *et al.*, The aged lymphoid tissue environment fails to support naïve T cell homeostasis. *Sci. Rep.* **6**, 30842 (2016).
6. A. Link *et al.*, Fibroblastic reticular cells in lymph nodes regulate the homeostasis of naive T cells. *Nat. Immunol.* **8**, 1255–1265 (2007).
7. K. Knoblich *et al.*, The human lymph node microenvironment unilaterally regulates T-cell activation and differentiation. *PLoS Biol.* **16**, e2005046 (2018).
8. Y. O. Alexandre, S. N. Mueller, Stromal cell networks coordinate immune response generation and maintenance. *Immunol. Rev.* **283**, 77–85 (2018).
9. Q. Qi, D. W. Zhang, C. M. Weyand, J. J. Goronzy, Mechanisms shaping the naïve T cell repertoire in the elderly–Thymic involution or peripheral homeostatic proliferation? *Exp. Gerontol.* **54**, 71–74 (2014).
10. R. E. Yanes, C. E. Gustafson, C. M. Weyand, J. J. Goronzy, Lymphocyte generation and population homeostasis throughout life. *Semin. Hematol.* **54**, 33–38 (2017).
11. J. Nikolich-Žugich, The twilight of immunity: Emerging concepts in aging of the immune system. *Nat. Immunol.* **19**, 10–19 (2018).
12. J. J. Goronzy, C. M. Weyand, Mechanisms underlying T cell ageing. *Nat. Rev. Immunol.* **19**, 573–583 (2019).
13. A. T. Krishnamurty, S. J. Turley, Lymph node stromal cells: Cartographers of the immune system. *Nat. Immunol.* **21**, 369–380 (2020).
14. H. L. Thompson *et al.*, Lymph nodes as barriers to T-cell rejuvenation in aging mice and nonhuman primates. *Aging Cell* **18**, e12865 (2019).

15. T. M. S. Kwok *et al.*, Age-associated changes to lymph node fibroblastic reticular cells. *Frontiers in Aging* (3):838943 (2022).
16. J. M. Richner *et al.*, Age-dependent cell trafficking defects in draining lymph nodes impair adaptive immunity and control of West Nile virus infection. *PLoS Pathog.* **11**, e1005027 (2015).
17. A. R. Masters *et al.*, Assessment of lymph node stromal cells as an underlying factor in age-related immune impairment. *J. Gerontol. A Biol. Sci. Med. Sci.* **74**, 1734–1743 (2019).
18. L. Lazuardi *et al.*, Age-related loss of naïve T cells and dysregulation of T-cell/B-cell interactions in human lymph nodes. *Immunology* **114**, 37–43 (2005).
19. J. L. Uhrlaub *et al.*, Dysregulated TGF-β production underlies the age-related vulnerability to Chikungunya virus. *PLoS Pathog.* **12**, e1005891 (2016).
20. A. R. Masters, E. R. Jellison, L. Puddington, K. M. Khanna, L. Haynes, Attrition of T cell zone fibroblastic reticular cell number and function in aged spleens. *Immunohorizons* **2**, 155–163 (2018).
21. J. S. Hale, T. E. Boursalian, G. L. Turk, P. J. Fink, Thymic output in aged mice. *Proc. Natl. Acad. Sci. U.S.A.* **103**, 8447–8452 (2006).
22. B. Zhang *et al.*, Glimpse of natural selection of long-lived T-cell clones in healthy life. *Proc. Natl. Acad. Sci. U.S.A.* **113**, 9858–9863 (2016).
23. K. Z. Martinet, S. Bloquet, C. Bourgeois, Ageing combines CD4 T cell lymphopenia in secondary lymphoid organs and T cell accumulation in gut associated lymphoid tissue. *Immun. Ageing* **11**, 8 (2014).
24. A. M. Wertheimer *et al.*, Aging and cytomegalovirus infection differentially and jointly affect distinct circulating T cell subsets in humans. *J. Immunol.* **192**, 2143–2155 (2014).
25. M. Czesnikiewicz-Guzik *et al.*, T cell subset-specific susceptibility to aging. *Clin. Immunol.* **127**, 107–118 (2008).
26. R. G. Scollay, E. C. Butcher, I. L. Weissman, Thymus cell migration. Quantitative aspects of cellular traffic from the thymus to the periphery in mice. *Eur. J. Immunol.* **10**, 210–218 (1980).
27. W. Yu *et al.*, Continued RAG expression in late stages of B cell development and no apparent re-induction after immunization. *Nature* **400**, 682–687 (1999).
28. D. C. Douek *et al.*, Changes in thymic function with age and during the treatment of HIV infection. *Nature* **396**, 690–695 (1998).
29. M. I. Harrell, B. M. Iritani, A. Ruddell, Lymph node mapping in the mouse. *J. Immunol. Methods* **332**, 170–174 (2008).
30. N. L. Tilney, Patterns of lymphatic drainage in the adult laboratory rat. *J. Anat.* **109**, 369–383 (1971).
31. J. G. Cyster, Chemokines, sphingosine-1-phosphate, and cell migration in secondary lymphoid organs. *Annu. Rev. Immunol.* **23**, 127–159 (2005).
32. C. Haluszczak *et al.*, The antigen-specific CD8+ T cell repertoire in unimmunized mice includes memory phenotype cells bearing markers of homeostatic expansion. *J. Exp. Med.* **206**, 435–448 (2009).
33. K. M. Quinn *et al.*, Age-related decline in primary $CD8^+$ T cell responses is associated with the development of senescence in virtual memory $CD8^+$ T cells. *Cell Rep.* **23**, 3512–3524 (2018).
34. K. R. Renkema, G. Li, A. Wu, M. J. Smithey, J. Nikolich-Žugich, Two separate defects affecting true naive or virtual memory T cell precursors combine to reduce naive T cell responses with aging. *J. Immunol.* **192**, 151–159 (2014).
35. B. D. Rudd *et al.*, Nonrandom attrition of the naive CD8+ T-cell pool with aging governed by T-cell receptor:pMHC interactions. *Proc. Natl. Acad. Sci. U.S.A.* **108**, 13694–13699 (2011).
36. V. Decman *et al.*, Defective CD8 T cell responses in aged mice are due to quantitative and qualitative changes in virus-specific precursors. *J. Immunol.* **188**, 1933–1941 (2012).
37. B. C. Chiu, B. E. Martin, V. R. Stolberg, S. W. Chensue, Cutting edge: Central memory CD8 T cells in aged mice are virtual memory cells. *J. Immunol.* **191**, 5793–5796 (2013).
38. D. G. Widman, T. Ishikawa, R. Fayzulin, N. Bourne, P. W. Mason, Construction and characterization of a second-generation pseudoinfectious West Nile virus vaccine propagated using a new cultivation system. *Vaccine* **26**, 2762–2771 (2008).
39. J. L. Uhrlaub, J. D. Brien, D. G. Widman, P. W. Mason, J. Nikolich-Zugich, Repeated in vivo stimulation of T and B cell responses in old mice generates protective immunity against lethal West Nile virus encephalitis. *J. Immunol.* **186**, 3882–3891 (2011).
40. J. D. Brien, J. L. Uhrlaub, J. Nikolich-Zugich, Protective capacity and epitope specificity of CD8(+) T cells responding to lethal West Nile virus infection. *Eur. J. Immunol.* **37**, 1855–1863 (2007).
41. P. J. Linton, K. Dorshkind, Age-related changes in lymphocyte development and function. *Nat. Immunol.* **5**, 133–139 (2004).
42. V. van Hoeven *et al.*, Dynamics of recent thymic emigrants in young adult mice. *Front. Immunol.* **8**, 933 (2017).
43. E. G. Houston Jr., R. Nechanitzky, P. J. Fink, Cutting edge: Contact with secondary lymphoid organs drives postthymic T cell maturation. *J. Immunol.* **181**, 5213–5217 (2008).
44. N. Watanabe *et al.*, Human thymic stromal lymphopoietin promotes dendritic cell-mediated CD4+ T cell homeostatic expansion. *Nat. Immunol.* **5**, 426–434 (2004).
45. A. Braun *et al.*, Afferent lymph-derived T cells and DCs use different chemokine receptor CCR7-dependent routes for entry into the lymph node and intranodal migration. *Nat. Immunol.* **12**, 879–887 (2011).
46. S. K. Bromley, S. Y. Thomas, A. D. Luster, Chemokine receptor CCR7 guides T cell exit from peripheral tissues and entry into afferent lymphatics. *Nat. Immunol.* **6**, 895–901 (2005).
47. T. H. Pham, T. Okada, M. Matloubian, C. G. Lo, J. G. Cyster, S1P1 receptor signaling overrides retention mediated by G alpha i-coupled receptors to promote T cell egress. *Immunity* **28**, 122–133 (2008).
48. J. S. Davies, H. L. Thompson, V. Pulko, J. Padilla Torres, J. Nikolich-Žugich, Role of cell-intrinsic and environmental age-related changes in altered maintenance of murine T cells in lymphoid organs. *J. Gerontol. A Biol. Sci. Med. Sci.* **73**, 1018–1026 (2018).
49. S. O. Alpdogan *et al.*, Rapidly proliferating CD44hi peripheral T cells undergo apoptosis and delay posttransplantation T-cell reconstitution after allogeneic bone marrow transplantation. *Blood* **112**, 4755–4764 (2008).
50. S. Dutta, P. Sengupta, Men and mice: Relating their ages. *Life Sci.* **152**, 244–248 (2016).
51. R. A. Miller, N. L. Nadon, Principles of animal use for gerontological research. *J. Gerontol. A Biol. Sci. Med. Sci.* **55**, B117–B123 (2000).
52. S. E. Fernandes, A. Alakesh, R. S. Rajmani, S. Jhunjhunwala, D. K. Saini, Aging associated altered response to intracellular bacterial infections and its implication on the host. *Biochim. Biophys. Acta Mol. Cell Res.* **1868**, 119063 (2021).
53. M. J. Smithey *et al.*, Lost in translation: Mice, men and cutaneous immunity in old age. *Biogerontology* **16**, 203–208 (2015).